INTERNATIONAL JOURNAL OF HYDROGEN ENERGY 46 (2021) 9514–9522

Available online at www.sciencedirect.com

ScienceDirect

journal homepage: www.elsevier.com/locate/he

Improving microbial electrolysis stability using flow-through brush electrodes and monitoring anode potentials relative to thermodynamic minima

Emmanuel U. Fonseca [a], *Kyoung-Yeol Kim* [b], *Ruggero Rossi* [a], *Bruce E. Logan* [a,*]

[a] *Department of Civil and Environmental Engineering, The Pennsylvania State University, 231Q Sackett Building, University Park, PA 16802, United States*

[b] *Department of Environmental and Sustainable Engineering, University at Albany, State University of New York, 1400 Washington Avenue, Albany, NY 12222, United States*

HIGHLIGHTS

- Forcing flow through single brush anode MECs produced highest performance.
- More stable current production in MEC with one compared to multiple brush anodes.
- More negative anode potential in MEC with flow forced through single anode.
- Higher energy efficiency in MEC with forced flow through a single anode.
- Anode potential data should be used in conjunction with current production data.

GRAPHICAL ABSTRACT

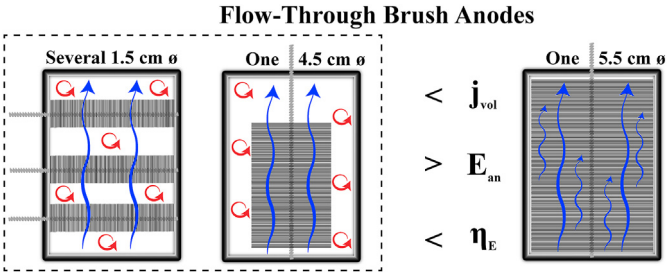

ARTICLE INFO

Article history:
Received 27 August 2020
Received in revised form
6 November 2020
Accepted 14 December 2020
Available online 6 January 2021

ABSTRACT

Graphite fiber brush electrodes are commonly used in microbial electrolysis cells (MECs) for simultaneous wastewater treatment and electrochemical hydrogen production. Previous brush anode designs for continuous flow systems were configured to have flow over an array of brush electrodes. Here we compared the performance of two systems, one with flow through a single smaller or larger brush anode to an MEC with multiple brushes. The single brush MECs had only a single large brush that had a diameter larger than the chamber height, so that the brush fibers were compressed to nearly (4.5 cm diameter) or completely (5.5 cm diameter) fill the 1.3 cm high anode chamber. To evaluate the time

* *Corresponding author.*
E-mail address: blogan@psu.edu (B.E. Logan).
https://doi.org/10.1016/j.ijhydene.2020.12.102

Keywords:
Microbial electrolysis cells
Hydrogen
Anode potential
Acclimation
Exoelectrogens
Graphite brush electrodes

needed for acclimation of the anode potentials were continuously monitored for 138 d (4.5 cm brush) or 143 d (5.5 cm brush). The best performance was obtained using the 5.5 cm brush fibers with a volumetric current density of 554 ± 26 A/m^3, compared to <400 A/m^3 when using the smaller 4.5 cm brush or the multiple brush reactor. Full acclimation was shown by a consistent and low anode potential, for example by −248 ± 8 mV (vs. a standard hydrogen electrode) for the 5.5 cm brush, which was only 31 ± 8 mV above the minimum estimated for acetate oxidation under standard biological conditions. These results show that brush compression into a smaller chamber can enhance MEC performance and produce anode potentials close the thermodynamic minima.

Introduction

The chemical energy content of domestic wastewater typically exceeds the energy used for traditional treatment more than 2-fold [41], presenting an opportunity for recovering this chemical energy during treatment. A microbial electrolysis cell (MEC) is a technology that can recover chemical energy by converting organic matter in wastewater into electrical current that is used to produce hydrogen gas [18,23,34,40,50]. The U.S. Department of Energy Fuel Cell Technology Office identified MECs as a critical technology for meeting H_2 cost goals from renewable biomass [45]. Although the overall reaction in an MEC is not spontaneous under desired operating conditions, the energy that is added into the system using an applied potential of 0.2–0.8 V is less than that used for water electrolysis (1.8–3.5 V) to produce H_2 [25]. Therefore, MECs used to treat wastewater can recover more energy as H_2 gas than that added to sustain current generation during operation [2,37].

Effective MEC scale-up requires reactor designs that can produce high current densities under continuous flow conditions. Volumetric current densities above 100 A/m^3 have been achieved using many different MEC designs and applied potentials [8,27,43,53]. One of the highest current densities (732 A/m^3) was achieved by continuously pumping the fluid through a thin felt anode [51]. However, the relatively high density of felt anodes may prohibit their use with wastewaters that contain particles as the anodes could clog. One alternative to felt anodes are graphite fiber brushes which have been shown to produce higher power densities in microbial fuel cells (MFCs) than felt electrodes [1,30,38]. For small MECs, a single brush is often used that partly fills the chamber [4,42]. Larger MECs, with continuous flow multiple brush anodes have been used with the size, number, and configuration of the graphite fibers showing mixed impacts on power production [6,10,29,31,44,48]. Despite the previous results showing good performance when the flow was forced through flat anodes, there have been no studies on using MECs or MFCs with the flow forced through a graphite fiber brush anode by using a brush with a larger diameter than that of the chamber.

Another factor important for overall MEC performance is the efficient recovery of H_2 gas. If a single-chamber MEC is used, with no membrane or separator between the electrodes, there can be H_2 gas recycling from the cathode to the anode which contributes to current generation but results in less net H_2 gas recovery [31,32,39]. In addition, the use of a single chamber can result in the loss of H_2 through its conversion to methane gas by methanogens. For example, in a very large MEC (1000 L), there was no H_2 gas recovery as all the gas extracted was methane [10]. Two-chamber reactor designs are considered to be essential for capture of H_2 from the cathode, and thus two-chamber MECs are increasingly used for wastewater treatment in bench- and pilot-scale MEC tests [9,19,22,28,36].

Consistent performance of MECs is important to show that the anodes are fully acclimated and that current generation is stable over time. However, the criteria to reach steady conditions are not well defined. In MECs acclimation times span days [1,8,10,20,24,46] to months [13,14,16,21,27,31,32,50]. At some point, when the reactor is considered to be acclimated, the performance is evaluated in terms of average current density or hydrogen gas production rates [3,7,15,17,34,43,44,51–54,56]. Steady conditions are typically defined as achieving some consistent current production over a limited period of operation. Often, steady conditions arise through consistent performance of the anodes, although anode potentials are not always continuously monitored and reported.

To improve MEC performance two different designs were examined here that used a single large brush, with a larger diameter than the height of the anode chamber, that was compared to the same chamber design equipped with several smaller brush anodes. A single large brush that was 4.5 cm in diameter was compressed to fit into the 1.3 cm high anode chamber, so that in mostly filled the width of the chamber (5.5 cm). To completely fill the anode chamber, the reactor was redesigned to contain a 5.5 cm brush so that the brush also was able to completely fill the chamber width. The anode potential was monitored in the single-brush reactors over time to better follow the acclimation of the anode and characterize exoelectrogenic microbial activity relative to overall performance based on current production [12,15,35,37,42,54,56,57]. The relationship between the theoretical oxidation potential for acetate oxidation and the anode potential was shown to be helpful for evaluating time to full acclimation. The

performance of the reactor relative to membrane fouling was also examined by replacing the membrane. Such information will help improve prospects for using MECs in wastewater treatment applications.

Materials and methods

MEC reactor configuration

The three-chambered MEC design (one anode chamber and two cathode chambers) used here provided additional cathode surface area by using two cathode chambers on either side of the brush anode chamber. The rectangular shaped anode chamber contained either multiple small brush anodes [1,27] or a large single brush anode (Fig. 1). The reactors were made of polycarbonate, with the anode chambers of the multiple brush anode MEC and the single 4.5 cm diameter brush anode MEC made of butyl rubber, while the 5.5 cm brush reactor was completely made of polycarbonate. The anode chambers (60 mL) had a 5.5 cm × 9.5 cm projected area but were only 1.3 cm in height, so that the larger single brush anodes were compressed when placed in the anode chamber. All graphite fiber brush anodes were made using two twisted titanium wires (Zoltec PX35 carbon fibers; Mill-Rose, Mentor, OH), with the anode and cathode chambers separated by an anion exchange membrane (AEM; Selemion AMV, AGC Engineering Co. Ltd., JP). The multiple anode MEC contained seven 4.5 cm × 1.5 cm brushes and had a total specific surface area (SSA) of 20.6 m^2 (Fig. 1A and D), with the anodes placed against the AEMs so the flow could occur around or through the brushes. The single brush anode MECs used either a smaller 7.5 cm long by 4.5 cm diameter brush (SSA = 12.0 m^2; Fig. 1B and E) or a larger 9.5 cm × 5.5 cm brush, with the brush compressed between the membranes to fit into the chamber (SSA = 18.6 m^2; Fig. 1C and F).

Each cathode chamber (35 mL) contained a stainless-steel wool cathode (316L SS, McMaster-Carr, USA) [27]. The cathode chambers each had one circular hole at the bottom and the top, allowing the catholyte to flow from bottom to top across each individual chamber. The multiple anode MEC and the 4.5 cm single anode MEC had one circular hole at the bottom and the top, while the 5.5 cm diameter brush anode chamber had two holes at the bottom and top to better distribute the influent flow. A reference electrode was inserted through a hole into both the 4.5 cm diameter single anode MEC (Ag/AgCl, model RE-5B, BASi, IN) and the 5.5 cm diameter single anode MEC (Ag/AgCl, model RRPEAGCL, Pine Research, NC).

MEC reactor operation

Voltage was added to the MEC circuit using a power supply (BK Precision, USA) set at 0.9 V (except as noted). The anolyte used in the multiple brush anode MEC was a synthetic fermentation effluent (1.2 g/L of chemical oxygen demand, COD) that consisted of sodium acetate (0.27 g), glucose (0.15 g), ethanol (0.11 g), lactic acid (0.07 g), and bovine serum albumin (BSA, 0.32 g) per liter of 50 mM phosphate buffer solution (PBS; 4.58 g Na_2HPO_4, 2.45 g NaH_2PO_4, 0.13 g KCl, and 0.31 g NH_4Cl in 1 L of deionized water) with mineral and vitamin solutions [27]. The anolyte used in the single brush anode MECs was an acetate buffer solution that consisted of sodium acetate (2 g/L; equivalent to 1.5 g/L of COD) dissolved in 50 mM PBS with mineral and vitamin solutions [49]. The catholyte contained only phosphate buffer (4.58 g Na_2HPO_4 and 2.45 g NaH_2PO_4) in 1 L of deionized water. The electrolytes were circulated through Viton tubing with a peristaltic pump set at flow rates of 40 mL/min (~1 min hydraulic retention time, HRT) for the catholytes and 10 mL/min (6 min HRT) for the anolyte. The electrolytes were recirculated from glass bottle reservoirs, 1 L for the anolyte and 0.5 L for each catholyte, through the

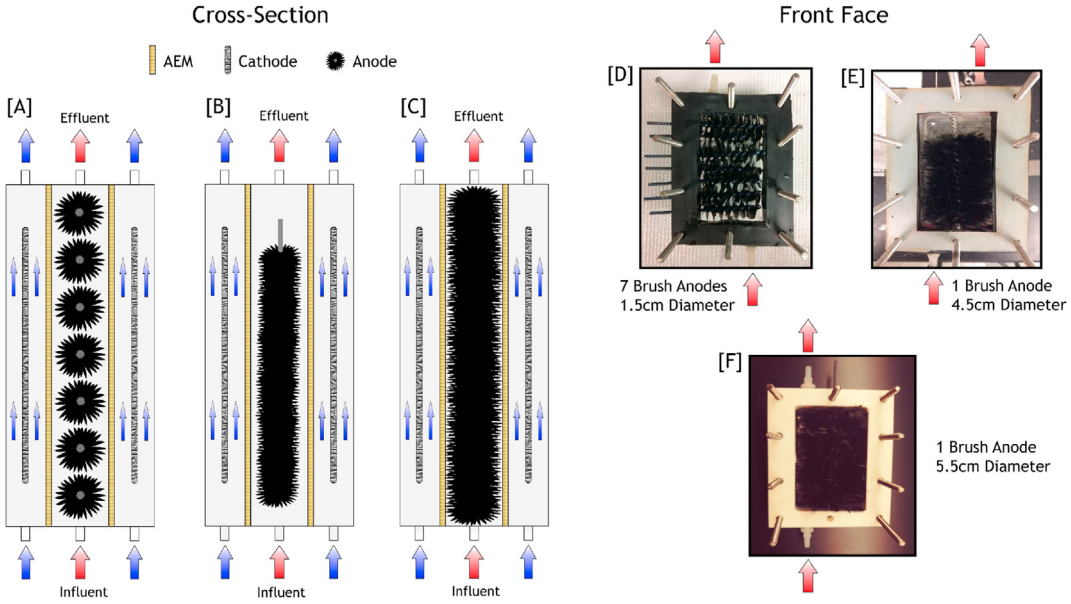

Fig. 1 – Continuous flow, graphite brush anode MEC designs. Graphics and photographs for the MEC with graphite brushes of (A, D) 1.5 cm diameter, (B, E) 4.5 cm diameter, and (C, F) 5.5 cm diameter. Arrows indicate the general direction of electrolyte flow.

reactor with the reservoirs sealed using gas tight rubber caps. The reservoirs were replenished with fresh media every 1–3 days. Prior to operation, fresh catholyte was deoxygenated by sparging the solutions with high purity nitrogen gas (99.998%) for 10–15 min with mixing using a magnetic bar. A gas collection bag (1 L, Calibrated Instruments, NY) was attached to each reservoir through the rubber cap to collect gases.

Current generation was monitored every 10 min by measuring the voltage across a 10 Ω resistor with a multimeter (Model 2700, Keithley Instruments, Inc., OH). Anode potential was monitored with the multimeter by measuring the potential between the anode and reference electrode. At the onset of each experiment, the anode was inoculated with effluent from a well-acclimated microbial fuel cell (50% anolyte buffer solution, 50% MFC effluent) for 7 days. After the inoculation period, only the anolyte buffer solution was fed into the anode chamber. Operation of the MEC with a single 5.5 cm diameter brush anode was temporarily suspended on day 41 of operation, and then filled with fresh electrolytes and stored in a refrigerated room (4 °C) for a few weeks, before being placed back into operation again (as indicated).

Theoretical anode potential calculations

Acetate oxidation by the half-cell reaction $CH_3COO^- + 4H_2O \rightarrow 2HCO_3^- + 9H^+ + 8e^-$ provides the energy that drives current generation in MECs [26,34]. The theoretical oxidation potential for acetate at non-standard conditions (E'_{an}) was calculated using the Nernst equation $E'_{an} = E^0_{an} - \frac{RT}{nF}\ln Q$, where $E^0_{an} = 0.187$ V, R is the gas law constant (8.314 J/K mol), T is the absolute temperature (293 K), F is Faraday's constant (96,485 C/mol), n is the number of electrons involved in the reaction (8 e^-), and Q is the reaction quotient. To calculate minimum anode potential we assumed pH = 7, $[HCO_3^-]$ = 5 mM, and $[CH_3COO^-]$ = 5 mM, resulting in $E'_{an} = -279$ mV vs. Standard Hydrogen Electrode (SHE) [37]. Calculations by others have yielded a similar value for the acetate oxidation thermodynamic minimum of −283 mV vs. SHE [47]. Measured anode potentials were then reported relative to this theoretical minimum as $\Delta E_{an} = E_{an} - E'_{an} = E_{an} + 279$.

Analytical measurements and calculations

A gas chromatograph (model 8610B, SRI Instruments Inc., USA) was used to analyze the composition of the gas collected from the gas bags and electrolyte reservoir headspaces. The volume of hydrogen produced in the gas bags was calculated based on adding a spike of high purity nitrogen gas to the gas bag following the initial analysis of the gas composition in the gas bag, as previously described [3]. The hydrogen production rate (L-H_2/L-reactor/d) was calculated based on the volume of hydrogen gas produced, total reactor volume (130 mL), and the total cycle time (~24 h). The COD of the reservoir electrolytes were measured before and after the cycle following standard methods (method 5220, HACH Company, CO). The Coulombic efficiency (C_e, %) was calculated based on the percent of current derived from the measured COD removed. The overall hydrogen yield (r_{H2}, %) was calculated as the percent of hydrogen recovered compared to the theoretical amount produced from measured COD removed. The energy yield relative to electrical input (η_E, %) was calculated based on recovered energy as H_2 compared to the electrical energy input needed to drive the endergonic electrolysis reactions. A thorough review of all calculated efficiencies can be found in Ref. [37]. Gas production analysis was only performed on the single 4.5 cm and 5.5 cm diameter graphite brush anode MECs.

All MEC performance data were normalized by the reactor volume (130 cm^3). Statistical significance of event performance impacts was calculated by two-tailed t-tests on the cycle (48 h) before and after the event of interest. Maximum current densities were calculated by averaging the absolute maximum current density with the maximum current density produced during the cycle (48 h) before and afterwards.

Results and discussion

MEC with a single 4.5 cm diameter graphite brush anode

The MEC with a single 4.5 cm diameter brush anode reached current densities of up to 200 A/m^3 within one day following inoculation (Fig. 2A). The current densities varied with each replacement of the electrolytes, with the maximum current achieved with fresh medium, and then the current gradually decreasing due to consumption of the substrate. In the initial cycles over the first 30 d the current densities ranged from 10 A/m^3 to >200 A/m^3, and then for the remainder of the operation time (days 30–138), the current densities were always above 140 A/m^3 with a maximum current density of 414 A/m^3.

Based on only current production, the MEC could have been considered to show stable performance based on reproducible cycles of current generation from days 35–60, and therefore considered to be fully acclimated. However, the anode potentials measured during this period suggested that the anode was not fully acclimated. The anode potentials remained mostly positive (vs. SHE) for a few weeks after the inoculation period (day 7–29), varying from 353 mV to −51 mV, with an average potential of 125 ± 63 mV (Fig. 2B). Based on this performance, the anode potential relative to the calculated thermodynamic minimum (ΔE_{an}) was 404 ± 63 mV. This is quite high relative to anode potentials in many other MEC and MFC studies where anodes typically have more negative potentials that are closer to the half-cell potential for acetate oxidation [49,56]. Between days 29 and 44, the anode potential continued to decrease with each cycle and became more negative, averaging −76 ± 60 mV (vs. SHE; ΔE_{an} of 203 ± 60 mV). This period of operation coincided with the emergence of even more homogeneous current production cycles.

The anode potential was maintained at fully negative potentials after day 44, and remained negative for the remainder of operation (days 44–138), averaging −194 ± 44 mV (vs. SHE), which was only ΔE_{an} = 85 ± 44 mV above the calculated minimum potential. These results suggest that an average ΔE_{an} of <100 mV may be required to observe uniform current production. Based on performance in anode potential, the time for acclimation took ~44 days.

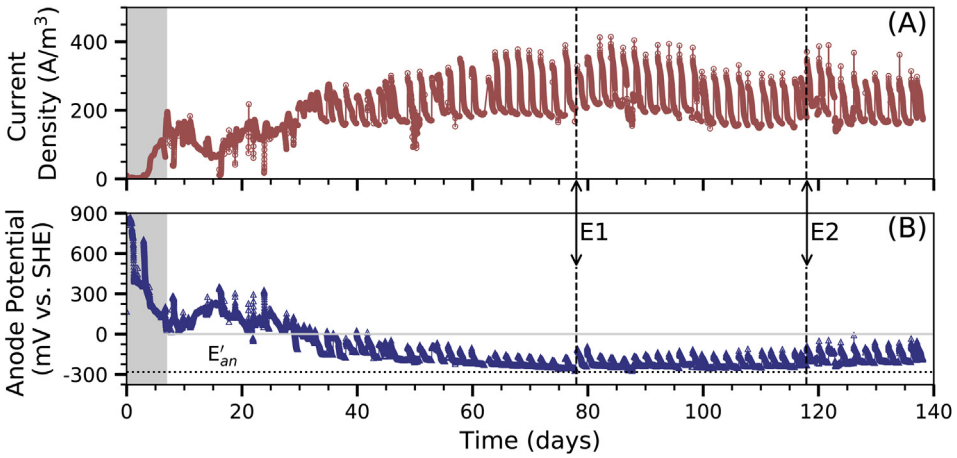

Fig. 2 – The performance of a single 4.5 cm diameter graphite brush anode MEC in current density (A) and anode potential (B). The period of anode inoculation is grayed out (days 0–7). The anode potential for acetate oxidation under standard biological conditions is −279 mV vs. SHE (B, dotted line). The anion exchange membranes were replaced at day 78 (E1). The applied potential was changed from 0.9 V to 1.0 V on day 118 (E2).

To examine the role of membrane fouling on MEC performance, the AEMs was replaced on day 78 (Fig. 2, point E1). After membrane replacement, the reactor's current production decreased significantly ($p < 0.001$) to a maximum current density of 330 A/m^3 compared to 389 A/m^3 before the change. Furthermore, the anode potential increased significantly ($p < 0.001$), to an average of −185 ± 47 mV (vs. SHE) compared to −227 ± 32 mV (vs. SHE) before AEM replacement. The decrease of current density and the increase of anode potential were most likely due to the exposure of oxygen to the anoxic electroactive microbes at the anode during the reactor disassembly. However, performance recovered quickly, and current production surpassed 400 A/m^3 within a few days of AEM replacement and reached maximum current density by day 84 (414 A/m^3). This increase in current density was likely due to a decrease in internal resistance when the AEMs were replaced.

To investigate if current densities could be increased further, the applied voltage was increased from 0.9 V on day 118 to 1.0 V (Fig. 2, point E2). Following the voltage increase, however, there was a negligible change in the current density ($p > 0.1$) with an average of 216 ± 48 A/m^3 (day 118–138) compared to 209 ± 49 A/m^3 (day 98–118) at 0.9 V. In contrast, the average anode potential increased significantly ($p < 0.001$), to −168 ± 43 mV (vs. SHE; day 118–138) compared to −211 ± 34 mV (vs. SHE; day 98–118) before the applied potential was increased. Increasing the applied potential from 0.9 V to 1.0 V therefore seemed to have little impact on current

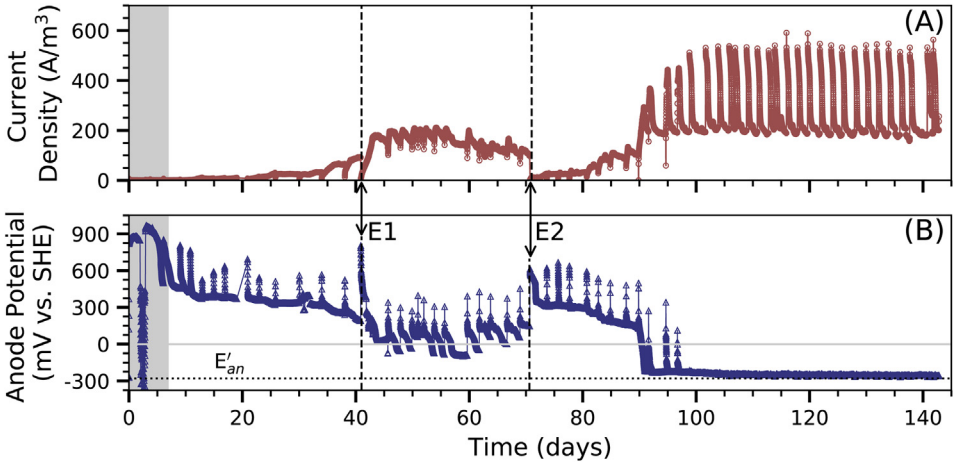

Fig. 3 – The performance of a single 5.5 cm diameter graphite brush anode MEC in current density (A) and anode potential (B). The period of anode inoculation is grayed out (days 0–7). The anode potential for acetate oxidation under standard biological conditions is −279 mV vs. SHE (B, dotted line). Operation was temporarily suspended, and the anion exchange membranes were replaced on day 41 (E1). At day 71, the anode brush was briefly extracted and rinsed with deionized water (E2).

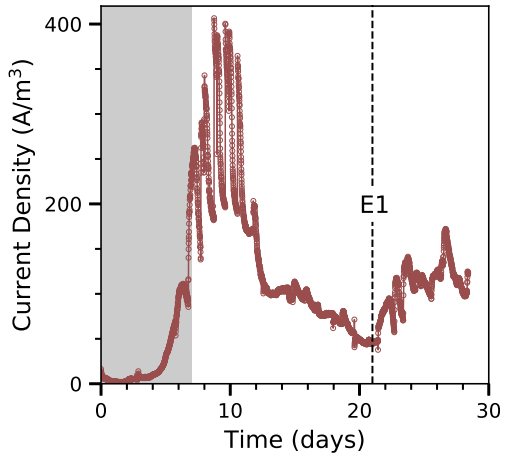

Fig. 4 – The performance of a seven 1.5 cm diameter graphite brush anode MEC in current density. The period of anode inoculation is grayed out (days 0–7). The reactor was re-inoculated at day 21 with MFC effluent (E1).

production but resulted in a 20% increase in anode potential. This deleterious effect of MEC operation at high applied voltages may be due to damage sustained by cells in the anodic biofilm at elevated voltages [11,33]. Other electrolysis integrated bioelectrochemical systems have shown effective operation at applied voltages >1.8 V [55] but very high voltages (3 V or 4 V) can result in damage to the biofilm by generation of chlorine gas due to chloride ion oxidation [5]. Typically applied voltages are kept ≤1 V to extract more energy in the hydrogen gas produced than the electrical energy added into the system [2,37].

MEC with a single 5.5 cm diameter graphite brush anode

The single large brush of 4.5 cm produced good performance but did not completely fill the width of the anode chamber, which may have allowed for some flow around the electrode. Therefore, the reactor was reconfigured so that a 5.5 cm diameter brush, that had the same width as the anode chamber, could be used to completely fill the chamber. The startup of the 5.5 cm diameter brush MEC was slower than the previous system, reaching a maximum current densities of <100 A/m^3 by day 40 (Fig. 3A). The lack of effective acclimation was also evident by the highly positive anode potentials (Fig. 3B), suggesting that reactor performance was largely due to the anode or some other factor impacting anode potentials. The AEMs were replaced on day 41 (Fig. 3, point E1) and current production reached 176 A/m^3, but this was associated with a significant ($p < 0.001$) increase in the anode potentials to 323 ± 145 mV (vs. SHE) compared to 224 ± 22 mV (vs. SHE) before AEM replacement. The current density then decreased to <100 A/m^3 by day 65 and < 70 A/m^3 by day 70.

One concern was that poor performance was due to possible biofilm clogging or anolyte flowing through a preferential flow path within the brush. For example, recent MFC experiments treating wastewater showed that larger diameter brush fiber anodes were more susceptible to clogging from biofilm growth, relative to smaller diameter brush fiber anodes [6]. Therefore, reactor operation was briefly suspended on day 71, and the anode was removed (Fig. 3, point E2). Visual inspection of the anode showed evidence of possible preferential flow paths (see SI), but little indication of clogging due to biofilm growth. The anode was then cleaned by gentle rinsing with deionized water, and then returned to operation.

After anode cleaning the performance based on current density continued to improve with each cycle, reaching >200 A/m^3 by day 90. Over each cycle the current densities ranged from 59 A/m^3 to >550 A/m^3, and for the remainder of operation (day 90–143), typically were always above 200 A/m^3 with a maximum current density of 554 ± 26 A/m^3. The improved performance was consistent with the development of highly negative anode potentials. The anode potentials were only fully negative relative after day 97, averaging −248 ± 8 mV (vs. SHE), or only $\Delta E_{an} = 31 \pm 8$ mV above the calculated minimum E'_{an}. This highly negative anode potential further supported the need to achieve anode potentials that have an ΔE_{an} of <100 mV. Based on the first batch cycle to operate at fully negative anode potentials, the time for acclimation took ~97 days.

MEC with seven 1.5 cm diameter graphite brush anodes

The MEC with seven graphite brush anodes initially produced high power densities, but current generation was not stable and decreased over time (Fig. 4). After 7 days the current densities reached more than 250 A/m^3, but then decreased to a range of ~140 A/m^3 to ~400 A/m^3 after 10 days of operation, and further declined to <120 A/m^3 by day 13 and < 50 A/m^3 by day 20. Re-inoculation of the reactor with effluent from an operating MFC (day 21, Fig. 4, point E1) temporarily increased

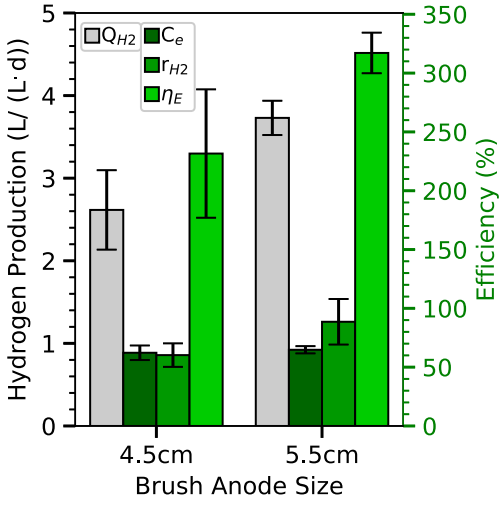

Fig. 5 – Hydrogen production rates (Q_{H2}) and efficiency analysis for the single graphite brush anode MECs tested. Coulombic efficiency (C_e), overall hydrogen recovery (r_{H2}), and the energy yield relative to electrical input (η_E) are shown. Error bars indicate standard deviation (4.5 cm brush n = 8; 5.5 cm brush n = 6).

the current density to 60–170 A/m^3 from day 21 to day 29, but the system thereafter failed to produce any stable or repeatable cycles of current generation. As a result of a lack of any stable operation, no further tests were conducted with the multi-brush anode MEC nor were anode potentials monitored as that capability had not been designed for this older reactor configuration.

Hydrogen production analysis

To ensure that the single graphite brush anode MECs were achieving their operational goal of recovering energy in the form of H_2 gas, we investigated H_2 production and energy impacts relative to the electrical inputs needed to prompt microbial electrolysis (Fig. 5). The 5.5 cm diameter brush anode MEC had the highest rate of 3.60 ± 0.31 L/L-d with a Coulombic efficiency of 64 ± 3%, an overall hydrogen recovery of 82 ± 22%, and an energy yield relative to electrical input of 317 ± 17%. The 4.5 cm diameter brush anode MEC produced 2.62 ± 0.48 L/L-d with a Coulombic efficiency of 62 ± 6%, an overall hydrogen recovery of 60 ± 10%, and an energy yield relative to electrical input of 232 ± 55%. The similar Coulombic efficiencies of both single brush anode reactors suggested that the cathodes behaved similarly regardless of the anode brush size; further implicating the importance of monitoring anode potential performance when comparing different MEC configurations. The improved performance of the larger brush anode reactor was likely a combined result of both the increase to anode size and the more complete filling of the chamber to avoid flow around the anode fibers. The hydrogen production analysis supports the energy positive impacts of operating single brush anode MECs.

Performance comparative analysis

Stable performance was observed in the single 5.5 cm diameter brush anode MEC, both in anode potential and current production. After the 97-day acclimation period, the anode potential averaged −248 ± 8 mV (vs. SHE; $\Delta E_{an} = 31 \pm 8$ mV) and current production cycles were markedly homogeneous with an average of 260 ± 102 A/m^3. The single 4.5 cm diameter brush anode MEC had stable performance after the 44-day acclimation period, with the anode potential averaging −194 ± 44 mV (vs. SHE; ΔE_{an} of 85 ± 44 mV) and homogeneous current production cycles averaging at 225 ± 53 A/m^3. This overall improvement to the performance of the 5.5 cm diameter brush anode MEC, particularly apparent in a comparison of anode potentials to the 4.5 cm diameter brush anode MEC, indicated a beneficial relationship between reactor stability and forcing more flow through brush anode fibers. In contrast to these single, larger brush experiments, the multiple brush anode MEC (seven 1.5 cm diameter brushes) did not reach stable current production. This comparison of single and multiple brush configurations therefore indicated that an MEC operating with a flow forced through larger brush anodes was more effective and stable than a reactor where flow can be carried around brush anodes.

Monitoring anode potential, rather than only current production, improved assessment of MEC acclimation times. Based on the first batch cycle to operate at fully negative anode potentials, the 5.5 cm diameter brush anode MEC took ~97 days to acclimate. This is a refinement over an estimate of the start-up period based on relatively stable current densities, which would have suggested acclimation within 45–95 days. Similarly, based on stable anode performance the 4.5 cm diameter brush anode MEC took ~44 days to acclimate. Previous studies have suggested acclimation times that are similar to those here [13,14,16,21,27,31,32,50], but many other studies have considered the reactors to be fully acclimated after < 30 days [1,8,10,20,46]. However, if the anode potentials had been reported in these studies, we believe better confirmation of the startup times would have been possible by examining whether ΔE_{an} was <100 mV or when the first batch cycle operated at fully negative anode potentials. By monitoring the anode potential here, it was possible to more accurately demonstrate the time needed for full acclimation.

Conclusions

Performance of continuous flow MECs with one graphite brush anode had improved stability in current production compared to a similar reactor containing multiple smaller graphite brush anodes. Forcing flow through the anode in single brush anode MECs improved the post-acclimation performance in both current production and anode potential, although performance during the start-up period was highly variable with acclimation periods ranging from 44 to 97 days. Analyzing anode potential during the reactor acclimation process helped quantify the approach to stable performance, thus improving metrics to predict the end of the start-up period and the potential for reactor destabilization.

Declaration of competing interest

The authors declare that they have no known competing financial interests or personal relationships that could have appeared to influence the work reported in this paper.

Acknowledgements

This work was conducted at the Pennsylvania State University and supported by funds provided by the US Department of Energy (DOE) Energy Efficiency and Renewable Energy (EERE) Fuel Cell Technologies Office, through a contract from the National Renewable Energy Laboratory (NREL), Project #21263.

Appendix A. Supplementary data

Supplementary data to this article can be found online at https://doi.org/10.1016/j.ijhydene.2020.12.102.

REFERENCES

[1] Ahn Y, Logan BE. A multi-electrode continuous flow microbial fuel cell with separator electrode assembly design. Appl Microbiol Biotechnol 2012;93:2241–8. https://doi.org/10.1007/s00253-012-3916-4.

[2] Aiken DC, Curtis TP, Heidrich ES. Avenues to the financial viability of microbial electrolysis cells [MEC] for domestic wastewater treatment and hydrogen production. Int J Hydrogen Energy 2019;44:2426–34. https://doi.org/10.1016/j.ijhydene.2018.12.029.

[3] Ambler JR, Logan BE. Evaluation of stainless steel cathodes and a bicarbonate buffer for hydrogen production in microbial electrolysis cells using a new method for measuring gas production. Int J Hydrogen Energy 2011;36:160–6. https://doi.org/10.1016/j.ijhydene.2010.09.044.

[4] Badia-Fabregat M, Rago L, Baeza JA, Guisasola A. Hydrogen production from crude glycerol in an alkaline microbial electrolysis cell. Int J Hydrogen Energy 2019;44:17204–13. https://doi.org/10.1016/j.ijhydene.2019.03.193.

[5] Baek G, Shi L, Rossi R, Logan BE. The effect of high applied voltages on bioanodes of microbial electrolysis cells in the presence of chlorides. Chem Eng J 2021;405:126742. https://doi.org/10.1016/j.cej.2020.126742.

[6] Brunschweiger S, Ojong ET, Weisser J, Schwaferts C, Elsner M, Ivleva NP, Haseneder R, Hofmann T, Glas K. The effect of clogging on the long-term stability of different carbon fiber brushes in microbial fuel cells for brewery wastewater treatment. Biores Technol Rep 2020;100420. https://doi.org/10.1016/j.biteb.2020.100420.

[7] Chacón-Carrera RA, López-Ortiz A, Collins-Martínez V, Meléndez-Zaragoza MJ, Salinas-Gutiérrez J, Espinoza-Hicks JC, Ramos-Sánchez VH. Assessment of two ionic exchange membranes in a bioelectrochemical system for wastewater treatment and hydrogen production. Int J Hydrogen Energy 2019;44:12339–45. https://doi.org/10.1016/j.ijhydene.2018.10.153.

[8] Clauwaert P, Verstraete W. Methanogenesis in membraneless microbial electrolysis cells. Appl Microbiol Biotechnol 2009;82:829–36. https://doi.org/10.1007/s00253-008-1796-4.

[9] Cotterill SE, Dolfing J, Curtis TP, Heidrich ES. Community assembly in wastewater-fed pilot-scale microbial electrolysis cells. Front Energy Res 2018;6:1–12. https://doi.org/10.3389/fenrg.2018.00098.

[10] Cusick RD, Bryan B, Parker DS, Merrill MD, Mehanna M, Kiely PD, Liu G, Logan BE. Performance of a pilot-scale continuous flow microbial electrolysis cell fed winery wastewater. Appl Microbiol Biotechnol 2011;89:2053–63. https://doi.org/10.1007/s00253-011-3130-9.

[11] Ding A, Yang Y, Sun G, Wu D. Impact of applied voltage on methane generation and microbial activities in an anaerobic microbial electrolysis cell (MEC). Chem Eng J 2015;283:260–5. https://doi.org/10.1016/j.cej.2015.07.054.

[12] Escapa A, Mateos R, Martínez EJ, Blanes J. Microbial electrolysis cells: an emerging technology for wastewater treatment and energy recovery. from laboratory to pilot plant and beyond. Renew Sustain Energy Rev 2016;55:942–56. https://doi.org/10.1016/j.rser.2015.11.029.

[13] Guo H, Kim Y. Stacked multi-electrode design of microbial electrolysis cells for rapid and low-sludge treatment of municipal wastewater. Biotechnol Biofuels 2019;12:1–10. https://doi.org/10.1186/s13068-019-1368-0.

[14] Guo H, Kim Y. Scalable multi-electrode microbial electrolysis cells for high electric current and rapid organic removal. J Power Sources 2018;391:67–72. https://doi.org/10.1016/j.jpowsour.2018.04.075.

[15] Hari AR, Katuri KP, Logan BE, Saikaly PE. Set anode potentials affect the electron fluxes and microbial community structure in propionate-fed microbial electrolysis cells. Sci Rep 2016;6:1–11. https://doi.org/10.1038/srep38690.

[16] Heidrich ES, Edwards SR, Dolfing J, Cotterill SE, Curtis TP. Performance of a pilot scale microbial electrolysis cell fed on domestic wastewater at ambient temperatures for a 12 month period. Bioresour Technol 2014;173:87–95. https://doi.org/10.1016/j.biortech.2014.09.083.

[17] Hu H, Fan Y, Liu H. Hydrogen production using single-chamber membrane-free microbial electrolysis cells. Water Res 2008;42:4172–8. https://doi.org/10.1016/j.watres.2008.06.015.

[18] Jafary T, Wan Daud WR, Ghasemi M, Abu Bakar MH, Sedighi M, Kim BH, Carmona-Martínez AA, Jahim JM, Ismail M. Clean hydrogen production in a full biological microbial electrolysis cell. Int J Hydrogen Energy 2019;44:30524–31. https://doi.org/10.1016/j.ijhydene.2018.01.010.

[19] Jain A, He Z. Powering microbial electrolysis cells by electricity generation from simulated waste heat of anaerobic digesters using thermoelectric generators. Int J Hydrogen Energy 2020;45:4065–72. https://doi.org/10.1016/j.ijhydene.2019.12.073.

[20] Jeremiasse AW, Hamelers HVM, Saakes M, Buisman CJN. Ni foam cathode enables high volumetric H_2 production in a microbial electrolysis cell. Int J Hydrogen Energy 2010;35(23):12716–23. https://doi.org/10.1016/j.ijhydene.2010.08.131.

[21] Jia YH, Ryu JH, Kim CH, Lee WK, Tran TVT, Lee HL, Zhang RH, Ahn DH. Enhancing hydrogen production efficiency in microbial electrolysis cell with membrane electrode assembly cathode. J Ind Eng Chem 2012;18:715–9. https://doi.org/10.1016/j.jiec.2011.11.127.

[22] Jayabalan T, Matheswaran M, Naina Mohammed S. Biohydrogen production from sugar industry effluents using nickel based electrode materials in microbial electrolysis cell. Int J Hydrogen Energy 2019;44:17381–8. https://doi.org/10.1016/j.ijhydene.2018.09.219.

[23] Jayabalan T, Matheswaran M, Preethi V, Naina Mohamed S. Enhancing biohydrogen production from sugar industry wastewater using metal oxide/graphene nanocomposite catalysts in microbial electrolysis cell. Int J Hydrogen Energy 2020;45:7647–55. https://doi.org/10.1016/j.ijhydene.2019.09.068.

[24] Jwa E, Yun YM, Kim H, Jeong N, Park SC, Nam JY. Domestic wastewater treatment in a tubular microbial electrolysis cell with a membrane electrode assembly. Int J Hydrogen Energy 2019;44:652–60. https://doi.org/10.1016/j.ijhydene.2018.11.036.

[25] Kadier A, Simayi Y, Abdeshahian P, Azman NF, Chandrasekhar K, Kalil MS. A comprehensive review of microbial electrolysis cells (MEC) reactor designs and configurations for sustainable hydrogen gas production. Alexandria Eng J 2016;55:427–43. https://doi.org/10.1016/j.aej.2015.10.008.

[26] Kadier A, Simayi Y, Kalil MS, Abdeshahian P, Hamid AA. A review of the substrates used in microbial electrolysis cells (MECs) for producing sustainable and clean hydrogen gas. Renew Energy 2014;71:466–72. https://doi.org/10.1016/j.renene.2014.05.052.

[27] Kim K-Y, Zikmund E, Logan BE. Impact of catholyte recirculation on different 3-dimensional stainless steel cathodes in microbial electrolysis cells. Int J Hydrogen Energy 2017;42(50):29708–15. https://doi.org/10.1016/j.ijhydene.2017.10.099.

[28] Korth B, Kuchenbuch A, Harnisch F. Availability of hydrogen shapes the microbial abundance in biofilm anodes based on

geobacter enrichment. ChemElectroChem 2020;1–6. https://doi.org/10.1002/celc.202000731.
[29] Lanas V, Ahn Y, Logan BE. Effects of carbon brush anode size and loading on microbial fuel cell performance in batch and continuous mode. J Power Sources 2014;247:228–34. https://doi.org/10.1016/j.jpowsour.2013.08.110.
[30] Lanas V, Logan BE. Evaluation of multi-brush anode systems in microbial fuel cells. Bioresour Technol 2013;148:379–85. https://doi.org/10.1016/j.biortech.2013.08.154.
[31] Lee HS, Rittmann BE. Significance of biological hydrogen oxidation in a continuous single-chamber microbial electrolysis cell. Environ Sci Technol 2010;44:948–54. https://doi.org/10.1021/es9025358.
[32] Lee HS, Torres CI, Parameswaran P, Rittmann BE. Fate of H_2 in an upflow single-chamber microbial electrolysis cell using a metal-catalyst-free cathode. Environ Sci Technol 2009;43:7971–6. https://doi.org/10.1021/es900204j.
[33] Lim SS, Fontmorin JM, Izadi P, Wan Daud WR, Scott K, Yu EH. Impact of applied cell voltage on the performance of a microbial electrolysis cell fully catalysed by microorganisms. Int J Hydrogen Energy 2020;45:2557–68. https://doi.org/10.1016/j.ijhydene.2019.11.142.
[34] Liu H, Grot S, Logan BE. Electrochemically assisted microbial production of hydrogen from acetate. Environ Sci Technol 2005;39:4317–20. https://doi.org/10.1021/es050244p.
[35] Liu H, Hu H, Chignell J, Fan Y. Microbial electrolysis: novel technology for hydrogen production from biomass. Biofuels 2010;1:129–42. https://doi.org/10.4155/bfs.09.9.
[36] Liu C, Sun D, Zhao Z, Dang Y, Holmes DE. Methanothrix enhances biogas upgrading in microbial electrolysis cell via direct electron transfer. Bioresour Technol 2019;291:121877. https://doi.org/10.1016/j.biortech.2019.121877.
[37] Logan BE, Call D, Cheng S, Hamelers HVM, Sleutels THJA, Jeremiasse AW, Rozendal RA. Microbial electrolysis cells for high yield hydrogen gas production from organic matter. Environ Sci Technol 2008;42:8630–40. https://doi.org/10.1021/es801553z.
[38] Logan B, Cheng S, Watson V, Estadt G. Graphite fiber brush anodes for increased power production in air-cathode microbial fuel cells. Environ Sci Technol 2007;41:3341–6. https://doi.org/10.1021/es062644y.
[39] Lu L, Hou D, Wang X, Jassby D, Ren ZJ. Active H_2 harvesting prevents methanogenesis in microbial electrolysis cells. Environ Sci Technol Lett 2016;3:286–90. https://doi.org/10.1021/acs.estlett.6b00209.
[40] Lu L, Ren ZJ. Bioresource Technology Microbial electrolysis cells for waste biorefinery : a state of the art review. Bioresour Technol 2016;215:254–64. https://doi.org/10.1016/j.biortech.2016.03.034.
[41] McCarty PL, Bae J, Kim J. Domestic wastewater treatment as a net energy producer-can this be achieved? Environ Sci Technol 2011;45:7100–6. https://doi.org/10.1021/es2014264.
[42] Nam JY, Tokash JC, Logan BE. Comparison of microbial electrolysis cells operated with added voltage or by setting the anode potential. Int J Hydrogen Energy 2011;36:10550–6. https://doi.org/10.1016/j.ijhydene.2011.05.148.
[43] Nam JY, Yates MD, Zaybak Z, Logan BE. Examination of protein degradation in continuous flow, microbial electrolysis cells treating fermentation wastewater. Bioresour Technol 2014;171:182–6. https://doi.org/10.1016/j.biortech.2014.08.065.
[44] Rader GK, Logan BE. Multi-electrode continuous flow microbial electrolysis cell for biogas production from acetate. Int J Hydrogen Energy 2010;35:8848–54. https://doi.org/10.1016/j.ijhydene.2010.06.033.
[45] Randolph K, Studer S. Biological hydrogen production workshop summary report. US Dep Energy, Off Energy Effic Renew Energy, Fuel Cell Technol Off; 2013. https://doi.org/10.1089/jmf.1998.1.65.
[46] Ribot-Llobet E, Nam JY, Tokash JC, Guisasola A, Logan BE. Assessment of four different cathode materials at different initial pHs using unbuffered catholytes in microbial electrolysis cells. Int J Hydrogen Energy 2013;38:2951–6. https://doi.org/10.1016/j.ijhydene.2012.12.037.
[47] Rittmann BE, McCarty PL. Table of Organic half-reactions and their Gibb's free energy. In: Environmental biotechnology: principles and applications. 2nd ed. McGraw-Hill Education; 2020.
[48] Rossi R, Cario BP, Santoro C, Yang W, Saikaly PE, Logan BE. Evaluation of electrode and solution area-based resistances enables quantitative comparisons of factors impacting microbial fuel cell performance. Environ Sci Technol 2019a;53:3977–86. https://doi.org/10.1021/acs.est.8b06004.
[49] Rossi R, Evans PJ, Logan BE. Impact of flow recirculation and anode dimensions on performance of a large scale microbial fuel cell. J Power Sources 2019b;412:294–300. https://doi.org/10.1016/j.jpowsour.2018.11.054.
[50] Rozendal RA, Hamelers HVM, Euverink GJW, Metz SJ, Buisman CJN. Principle and perspectives of hydrogen production through biocatalyzed electrolysis. Int J Hydrogen Energy 2006;31:1632–40. https://doi.org/10.1016/j.ijhydene.2005.12.006.
[51] Sleutels THJA, Lodder R, Hamelers HVM, Buisman CJN. Improved performance of porous bio-anodes in microbial electrolysis cells by enhancing mass and charge transport. Int J Hydrogen Energy 2009;34:9655–61. https://doi.org/10.1016/j.ijhydene.2009.09.089.
[52] Sun D, Cheng S, Zhang F, Logan BE. Current density reversibly alters metabolic spatial structure of exoelectrogenic anode biofilms. J Power Sources 2017;356:566–71. https://doi.org/10.1016/j.jpowsour.2016.11.115.
[53] Tartakovsky B, Manuel MF, Wang H, Guiot SR. High rate membrane-less microbial electrolysis cell for continuous hydrogen production. Int J Hydrogen Energy 2009;34:672–7. https://doi.org/10.1016/j.ijhydene.2008.11.003.
[54] Wang A, Liu W, Ren N, Zhou J, Cheng S. Key factors affecting microbial anode potential in a microbial electrolysis cell for H_2 production. Int J Hydrogen Energy 2010;35:13481–7. https://doi.org/10.1016/j.ijhydene.2009.11.125.
[55] Ye B, Luo H, Lu Y, Liu G, Zhang R, Li X. Improved performance of the microbial electrolysis desalination and chemical-production cell with enlarged anode and high applied voltages. Bioresour Technol 2017;244:913–9. https://doi.org/10.1016/j.biortech.2017.08.049.
[56] Zakaria BS, Lin L, Dhar BR. Shift of biofilm and suspended bacterial communities with changes in anode potential in a microbial electrolysis cell treating primary sludge. Sci Total Environ 2019;689:691–9. https://doi.org/10.1016/j.scitotenv.2019.06.519.
[57] Zhang Y, Angelidaki I. Microbial electrolysis cells turning to be versatile technology: Recent advances and future challenges. Water Res 2014;56(0):11–25.